

Soundscape modelling in a marine area designated for floating offshore wind turbine (FOWT) development in northern Portugal

Marcos Ricardo Souza¹, Tiago Gomes¹, Guilherme Vaz^{1,2}

¹blueOASIS, Portugal

²University of Southampton, United Kingdom

Marcos Ricardo Souza. Rua do Norte, 16, 2655-321, Ericeira, Portugal.
msouza@blueoasis.pt

Abstract: *Environmental impact assessment and planning are crucial in offshore energy production, where underwater acoustics play a key role. As wind turbines generate energy, vibrations from moving components in the generator are also produced. These vibrations travel through the structure and are finally radiated to the underwater environment. Building on the FLOATFARM project, this study develops sound maps incorporating various anthropogenic sources for Viana do Castelo, Portugal, where floating offshore wind farms are planned. The Source Level of an individual floating wind turbine (FOWT) is estimated using Finite Element Analysis based on structural vibrations. Acoustic-structure interaction is considered, and radiated power is computed to calculate the acoustic Source Level. Underwater noise propagation is then modelled using blueOASIS's RAINDROP, a tool that streamlines noise map creation. The model integrates site-specific bathymetry and AIS data to account for vessel contributions to the soundscape, alongside the windfarms and multiple FOWTs. Results include SPL levels around the wind farms at assumed different power generation conditions. Further advancements are needed in powertrain modelling and vibration and acoustic data validation. Nevertheless, this study proposes a framework for characterizing FOWT structure-borne noise and its underwater propagation, contributing to a more comprehensive understanding of offshore wind farm acoustics, even during project design stages.*

Keywords: *Underwater Acoustics, Floating Offshore Windfarm, Renewables, RAINDROP*

1. INTRODUCTION

In 1990, Sweden installed the world's first offshore wind turbine [1], marking the start of a rapidly advancing field in renewable energy. The 1990s also marked the starting point of floating offshore wind turbine research [2]. While most of the operational offshore wind turbines are bottom-fixed structure[1], it is expected that the 2023 capacity of 121 MW [2] will have increased to 264 GW by 2050 [3].

Floating offshore wind farm development presents many advantages over bottom-fixed (or onshore) windfarms, such as extended water depth range [4], [5], insensitivity to seabed properties [5], invisibility [6](avoiding the “not in my backyard” problem). However, they still affect their environment and require detailed planning and environmental impact assessments. The work presented in this paper aims at helping facilitate these assessments by providing a framework for numerical simulations that can quantify the underwater acoustic impact due to floating offshore windfarms also combining it with shipping noise. The methodology is applied to a windfarm (800 MW) planned for Viana do Castelo, in the north of Portugal, shown in Fig. 1.



Fig. 1: Portugal and the planned Viana do Castelo wind farm area.

The paper is organised as follows: section 2 covers the source characterisation and underwater sound propagation; section 3 presents the results; section 4 provides the final remarks.

2. NUMERICAL MODELLING

For the underwater soundscape analysis, it is first required to establish the source characteristics. This is done via a finite element model of a single floating offshore wind turbine, where its Source Level (SL) is estimated from the calculated radiated sound power W . After the source is characterised, noise propagation maps are calculated considering multiple wind turbines and shipping traffic. The methodology is shown schematically in Fig. 2.

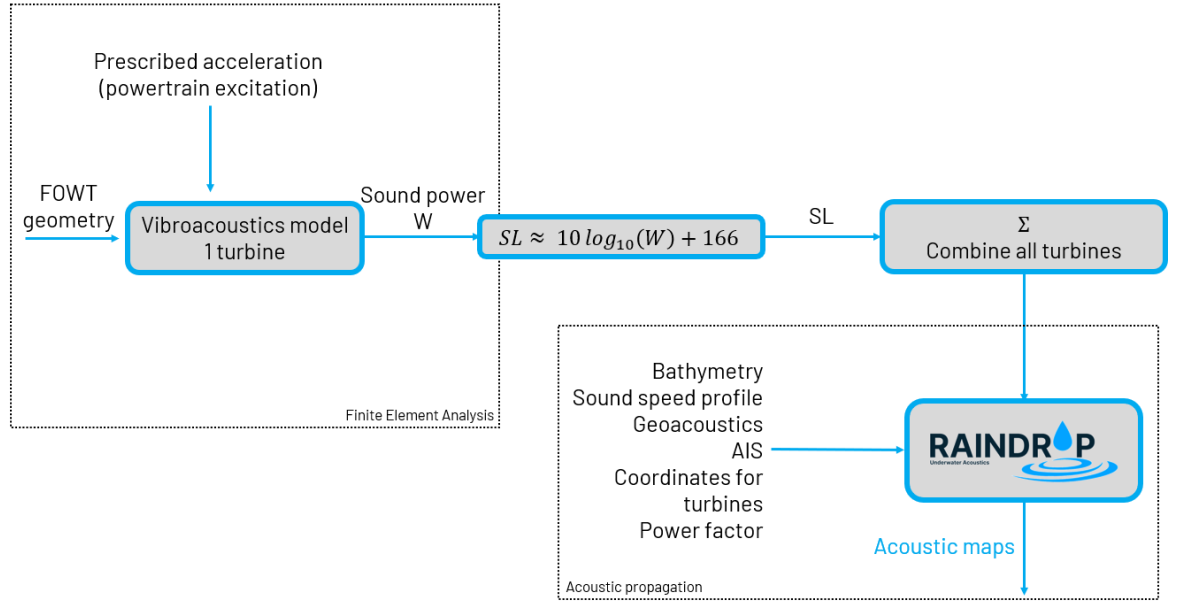


Fig. 2: Methodology overview.

2.1. Finite element analysis: source characterisation

The model was built in COMSOL 6.3 using an axisymmetric shell representing a spar-type substructure, such as the Hywind wind turbine [7]. Structural steel properties were used, with a damping ratio of 0.001. The thickness of the shell varies from 19 mm to 27mm. The diameter at the top of the tower is 6.5m and 7.5 where it connects to the spar buoy. For the floater, the diameter varies from 14.4 m at its lowest point to 7.5 m. The *Pressure Acoustics, Frequency Domain* physics is combined with the structural *Shell* physics via the *Acoustic-Structure Interaction* multiphysics, following Eqs. (1)-(2) [8]:

$$-\mathbf{n} \left(-\frac{1}{\rho_c} \nabla p_t \right) = -\mathbf{n} \mathbf{u}_{tt} \quad (1)$$

$$\mathbf{F}_A = p_t \mathbf{n} \quad (2)$$

where \mathbf{n} is the surface normal, ρ_c is the fluid density (water in this case), p_t is the total acoustic pressure, \mathbf{u}_{tt} is the out-of-plane surface acceleration of the structure and \mathbf{F}_A is the force per unit area experienced by the structure.

A radial acceleration mimicking the excitation from the powertrain is prescribed at the top of the tower. The water domain size changes with the frequency being analysed in order to accommodate at least 3 wavelengths, aiming at having free field propagation. The air-water interface is modelled as a soft boundary, meaning that the pressure vanishes at the interface; and perfectly matched boundary is set at the other water boundaries. This avoids reflections at the boundaries, creating anechoic boundaries. The meshed model is shown in Fig. 3(a).

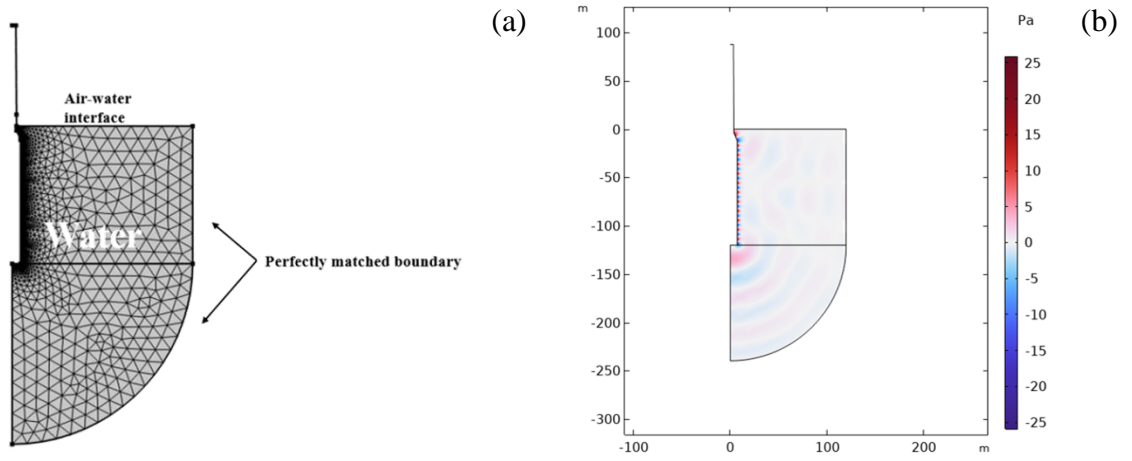


Fig. 3: Meshed model in (a) and acoustic pressure at 40Hz in (b)

Vibroacoustic data for offshore wind turbine is scarce in the literature, especially for floating ones. The excitation at the top of the tower was based on the report of Lindell [9], that has the radial acceleration of the structure at points close to the water surface. A unit-amplitude broadband acceleration was first applied at the tower top in the finite element model. The resulting acceleration was computed at a point 10 meters above sea level. This allowed the derivation of a transfer function between the top prescribed acceleration and the response down the structure. Using this transfer function in conjunction with the measured acceleration spectrum from Lindell, an equivalent prescribed spectrum was inferred that would produce comparable radial acceleration levels in the numerical model. An example of the resulting acoustic pressure is shown in Fig. 3(b).

COMSOL also provides the radiated sound power. This is converted to Source Level with the following assumptions: the equivalent source is a monopole at a depth greater than 1 m and at more than 1 m from the seafloor. Meaning that SL will be estimated as the sound pressure level at 1 m from the monopole source based on the area of a 1 m radius sphere and the calculated sound power. Therefore, the following can be written [10],

$$W = IA = \frac{p^2}{\rho c} A \quad (3)$$

$$p^2 = \frac{W \rho c}{4\pi} \quad (4)$$

where W is the radiated sound power, I is the sound intensity, A is the area of the unit sphere 4π , p is the acoustic pressure, ρ is the water density and c is the water speed of sound. Moreover,

$$SPL = 10 \log_{10}(p^2/p_{ref}^2), p_{ref} = 10^{-6} Pa. \quad (5)$$

Therefore, at 1 m,

$$SL = 10 \log_{10}(p^2) - 10 \log_{10}(p_{ref}^2) \quad (6)$$

$$SL = 10 \log_{10}(W) + 10 \log_{10}(\rho c) - 10 \log_{10}(4\pi) - 20 \log_{10}(p_{ref}) \quad (7)$$

$$SL \approx 10 \log_{10}(W) + 61.8 - 15.9 + 120 \approx 10 \log_{10}(W) + 166 \quad (8)$$

2.2. Sound propagation

RAINDROP¹ is a holistic framework for computational ocean acoustics, developed by blueOASIS, that targets Digital Twins of the Ocean applications. It seamlessly integrates Python code with extensively validated acoustic propagation solvers. In this paper, KRAKEN [11] was used as the propagation solver. It can efficiently process complex marine data, including bathymetry, metocean information, and ship AIS data, along with custom acoustic sources, such as wind farms.

The bathymetry data was obtained from EMODnet [12], while the water properties to calculate the sound speed profile come from the Atlantic-Iberian Biscay Irish-Ocean dataset [13], following the UNESCO formula [14], both shown in Fig. 4. For convenience, the SSP was obtained for the point at the greatest depth and averaged for the month of December 2024. Also, the seafloor was considered to have uniform geoacoustic properties summarised in Table 1 [15]. However, RAINDROP accepts different properties in a similar fashion to bathymetry. Based on the AIS data, the SL of any vessels presenting in the area of interest are automatically calculated by the toolbox based on the JOMOPANS-ECHO model [16].

For the anticipated capacity of 800 MW and considering that each Hywind turbine has a capacity of 6MW, the Viana do Castelo wind farm would need 134 turbines.

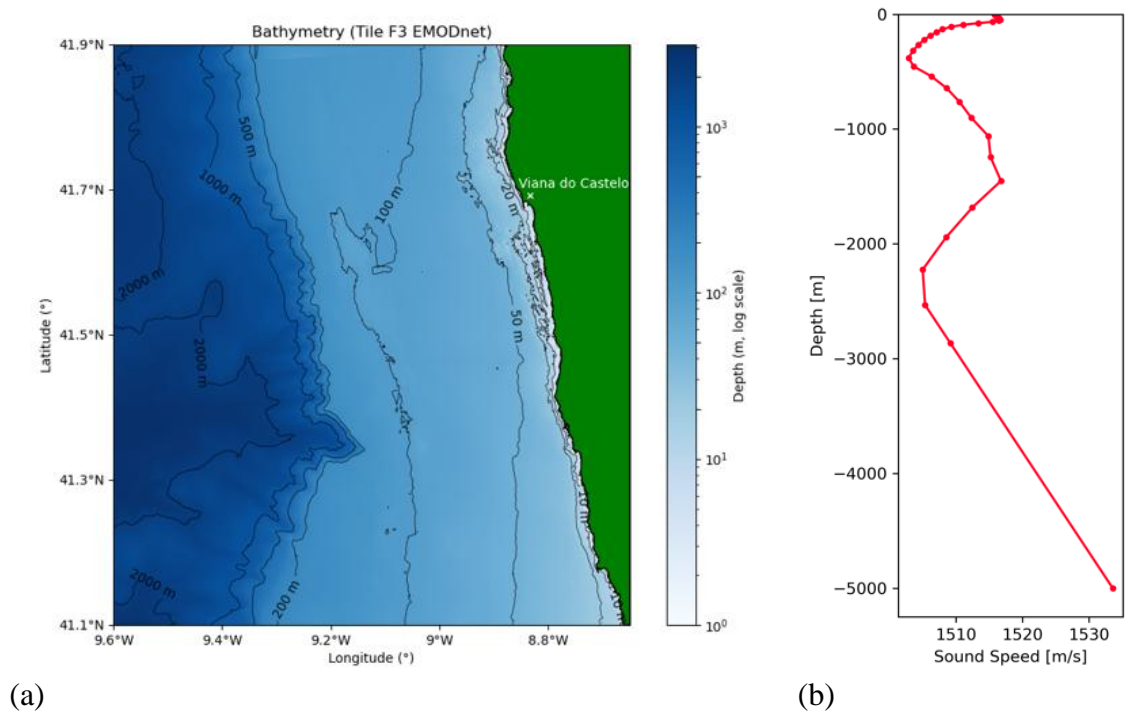


Fig. 4: RAINDROP inputs – in (a), bathymetry and in (b) sound speed profile

¹ <https://blueoasis.pt/raindrop/>

Property	Value
Density [g/cm ³]	2.1
P-wave speed [m/s]	1885
S-wave speed [m/s]	0
P-wave attenuation [dB]	34
S-wave attenuation [dB]	25

Table 1: Geoacoustic properties of the seabed

3. RESULTS

The EU Marine Strategy Framework Directive recommends assessing the 63 Hz and the 125 Hz third-octave frequency bands for environmental impact of shipping noise. The results presented in this paper are for the 63 Hz band.

Firstly, to help define the baseline of the soundscape, RAINDROP was run without the windfarm (marked by the light grey polygon), to assess the impact of shipping traffic. For a randomly selected instant in time, the map is produced, with three fishing vessels and a bulker from the AIS available. The map is shown in Fig. 6. The “louder” bulker produces SPL close to 150 dB close to it, but with most of the noise being between 100-120 dB, concentrated in an area with a radius of around 15 km.

The transfer function $H = a_{down}/a_{top}$ between the prescribed acceleration at top and the acceleration 10 m from the water surface is shown in Fig. 5. These are accelerations in the radial direction of the structure. As discussed previously, this was constructed from a unit acceleration first, which was then used to adjust the prescribed acceleration at the top in order to obtain similar levels of acceleration reported in the literature closer to the water surface.

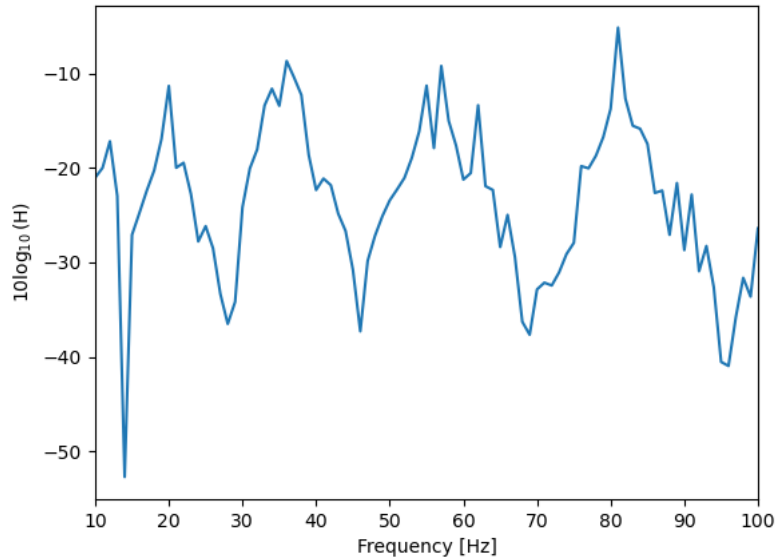


Fig. 5: Acceleration transfer function.

The structural model for the tower, at the 63 Hz, calculates an acceleration of around 0.02 m/s². The calculated sound power is 0.0479 W, leading to a SL estimation of 152.6 dB re 1 μPa @ 1 m. Literature reports measured median SL between 149-155 dB re 1 μPa @ 1 m [17] for the Hywind project at 63 Hz depending on the wind speed. However, it is

important to note that the results in literature include additional noise sources such as the moorings. These are expected to contribute more at higher frequencies, but might have some influence at this particular band, as well. Moreover, the highest SL measured occurs at 80 Hz. Regardless, the proposed methodology produces comparable SL and with adjusted input excitation, better agreement is expected. The map with the windfarm and shipping traffic is shown in Fig. 7.

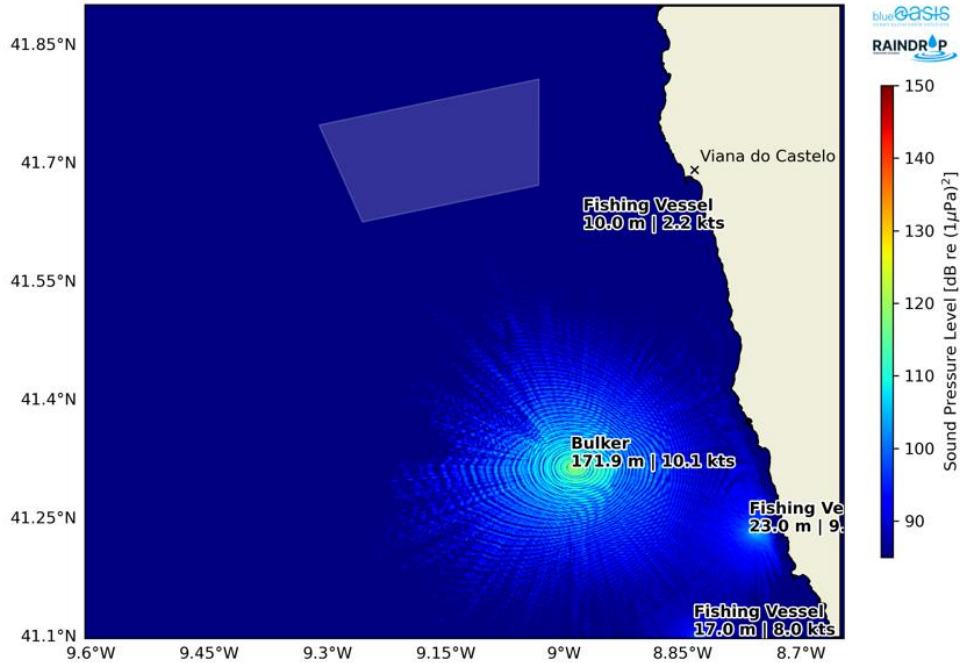


Fig. 6: Acoustic map at 63 Hz with vessels in the Viana do Castelo area.

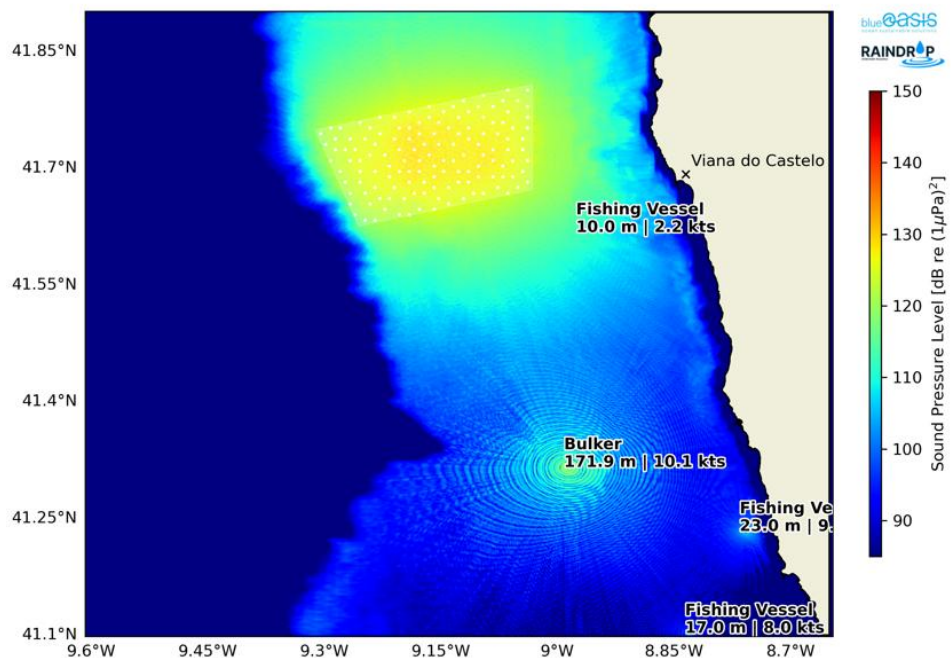


Fig. 7: Acoustic map at 63Hz considering the planed 800 MW windfarm and shipping.

The results consider that all of 134 turbines are a monopole with a SL of 152.6 dB re 1 μ Pa @ 1 m. This leads to similar SPL from the bulker, also extending more than 15 km

from the windfarm, but in a more uniform area. It stands to reason that the SL will be proportional to the operating condition of the turbine and therefore it is unlikely that all of them are under the same condition. This means that in the real operation, some fluctuation will be present. Moreover, the prescribed acceleration at the top of the tower is not validated, which might lead to deviations in the calculated of the SL. The windfarm operating at different conditions is also shown in Fig. 8. Note the power factor turbine $p_{fac.turb}$ percentage. The calculated radiated sound power W in these cases is directly multiplied by this value. Therefore, if it says 9%, the estimated W is multiplied by 0.09 leading to a SL of 142.1 dB re 1 μ Pa @ 1 m.

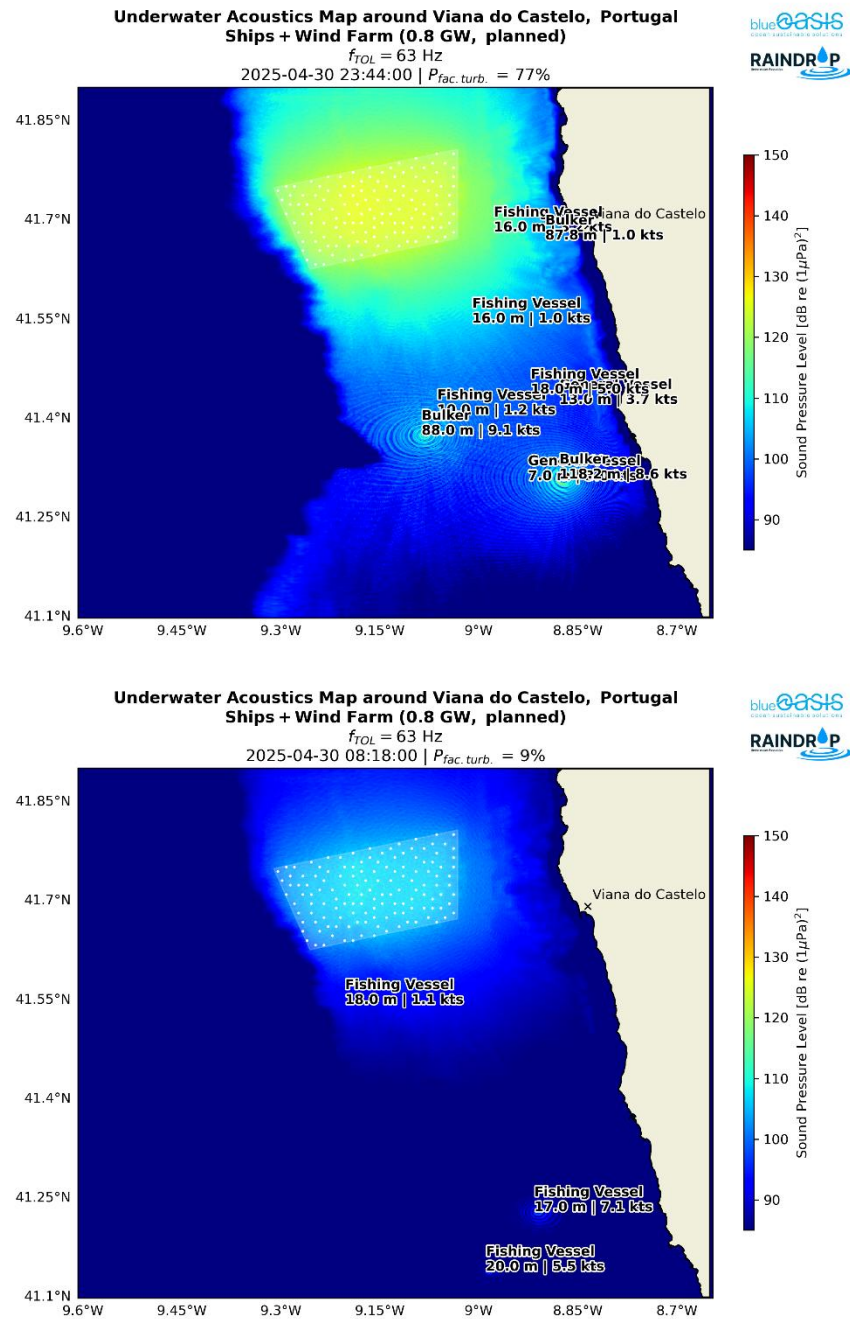


Fig. 8: Windfarm at different operating conditions and different vessels in the area

4. FINAL REMARKS

This paper presents a methodology for estimating the underwater acoustic impact of floating offshore wind turbines and wind farms, starting from finite element modeling and extending to acoustic propagation analysis. This approach helps to enable effective planning and environmental impact assessments, as well as guidance on noise mitigation strategies.

A single turbine is first modeled to estimate its Source Level based on radiated sound power derived from the finite element simulation. Once characterized, this source can be replicated across the planned wind farm layout. By integrating this with established underwater acoustic solvers, the overall acoustic footprint of the wind farm is calculated. Results show that the SPL footprint of the wind farm can be comparable to shipping traffic and can extend to a larger area. However, the actual impact for a real operating wind turbine requires further validation, due to the uncertainty in the excitation from the generator. Regardless of challenges in defining model inputs, the estimated SL is within the range of available experimental data. Therefore, the methodology holds just requiring fine tuning of the input data. The results shown here also consider that every wind turbine is operating with the same condition and therefore has the same SL. This can be changed in RAINDROP with either the use of a power factor that changes the SL depending on the operating conditions of each specific turbine or the farm as a whole.

RAINDROP can also provide results in terms of other quantities such as Level of Onset of Biological Adverse Effects, LOBE. Future work will focus on simulating the wind-loaded generator powertrain for more accurate excitation modeling and employing reduced-order modeling techniques to accommodate more complex turbine geometries beyond the axisymmetric model used in this study and different vibroacoustics modelling, such as Statistical Energy Analysis.

ACKNOWLEDGEMENTS

This research is part of the FLOATFARM project, funded by the European Union under the Horizon Europe programme Grant Agreement No. 101136091. The authors also acknowledge the University of Southampton for providing access to essential software resources and Marine Traffic for their AIS trial.

REFERENCES

- [1] M. Barooni, T. Ashuri, D. Velioglu Sogut, S. Wood, and S. Ghaderpour Taleghani, "Floating Offshore Wind Turbines: Current Status and Future Prospects," *Energies*, vol. 16, no. 1, Art. no. 1, Jan. 2023, doi: 10.3390/en16010002.
- [2] "Evolution of floating offshore wind platforms: A review of at-sea devices," *Renewable and Sustainable Energy Reviews*, vol. 183, p. 113416, Sep. 2023, doi: 10.1016/j.rser.2023.113416.
- [3] "DNV: Floating offshore wind: The next five years," DNV, 2022.
- [4] "Economic feasibility of floating offshore wind farms," *Energy*, vol. 112, pp. 868–882, Oct. 2016, doi: 10.1016/j.energy.2016.06.135.

- [5] “Technical and economic aspects of a floating offshore wind farm,” *Journal of Wind Engineering and Industrial Aerodynamics*, vol. 74–76, pp. 399–410, Apr. 1998, doi: 10.1016/S0167-6105(98)00036-1.
- [6] P. Sclavounos, “Floating Offshore Wind Turbines,” *Marine Technology Society Journal*, vol. 42, no. 2, pp. 39–43, Jun. 2008, doi: 10.4031/002533208786829151.
- [7] K. E. Steen, “Hywind Scotland – status and plans – Statoil,” presented at the EERA DeepWind’ 2016, Trondheim, Norway, 2016.
- [8] “COMSOL Acoustics Module User’s Guide.” COMSOL. Accessed: May 26, 2025. [Online]. Available: <https://doc.comsol.com/5.4/doc/com.comsol.help.aco/AcousticsModuleUsersGuide.pdf>
- [9] H. Lindell, *Utgrunden off-shore wind farm - Measurements of underwater noise*. 2003.
- [10] F. Fahy, “Sound Energy and Intensity,” in *Foundations of Engineering Acoustics*, Academic Press, 2001, pp. 74–95. doi: 10.1016/B978-012247665-5/50006-0.
- [11] M. B. Porter, “The KRAKEN normal mode program,” *SACLANT Undersea Research Centre Memorandum (SM-245)*, 1991, Accessed: May 26, 2025. [Online]. Available: <https://ui.adsabs.harvard.edu/abs/1992knmp.book.....P/abstract>
- [12] “EMODnet Map Viewer.” Accessed: May 27, 2025. [Online]. Available: <https://emodnet.ec.europa.eu/geoviewer/>
- [13] Copernicus, “Atlantic-Iberian Biscay Irish- Ocean Physics Analysis and Forecast.” Accessed: May 27, 2025. [Online]. Available: https://data.marine.copernicus.eu/product/IBI_ANALYSISFORECAST_PHY_005_001/description
- [14] C.-T. Chen and F. J. Millero, “Speed of sound in seawater at high pressures,” *The Journal of the Acoustical Society of America*, vol. 62, no. 5, pp. 1129–1135, Nov. 1977, doi: 10.1121/1.381646.
- [15] P. Pregitzer, “Underwater Acoustic Impact of Marine Renewable Energy Devices: Modelling Approaches,” Master of Science, Instituto Superior Técnico, Lisboa, Portugal, 2021.
- [16] A. MacGillivray and C. De Jong, “A Reference Spectrum Model for Estimating Source Levels of Marine Shipping Based on Automated Identification System Data,” *JMSE*, vol. 9, no. 4, p. 369, Mar. 2021, doi: 10.3390/jmse9040369.
- [17] F. Pace *et al.*, “Underwater Sound Emissions from the Moorings of Floating Wind Turbines: HYWIND Scotland Case Study,” in *The Effects of Noise on Aquatic Life: Principles and Practical Considerations*, A. N. Popper, J. A. Sisneros, A. D. Hawkins, and F. Thomsen, Eds., Cham: Springer International Publishing, 2024, pp. 179–201. doi: 10.1007/978-3-031-50256-9_121.